

Thermal properties of blends comprising poly(3-hydroxybutyrate-*co*-3-hydroxyvalerate) and epoxidized natural rubber

C. H. Chan · H. W. Kammer

Received: 16 November 2008 / Revised: 12 February 2009 / Accepted: 21 April 2009 /
Published online: 28 May 2009
© Springer-Verlag 2009

Abstract Blends of poly(3-hydroxybutyrate-*co*-3-hydroxyvalerate) (PHBV) with 12 mol% hydroxyvalerate (HV) content and epoxidized natural rubber (ENR) with 50 mol% epoxidation level were studied along with the thermal properties and morphologies. Glass transition temperatures reveal immiscibility of the polymers over the entire composition range. The equilibrium melting point (T_m^0) of PHBV in blends was determined applying Hoffman–Weeks step-wise annealing procedure. There is no significant variation of T_m^0 for PHBV with blend composition. Also the crystallinity of PHBV stays approximately constant in the blends, only a slight decrease might be recognized with increasing ENR content. The rate of crystallization of PHBV decreases with PHBV content according to a power law. Morphological studies by polarizing optical microscopy reveal a fine intraspherulitic dispersion of ENR in volume-filling PHBV spherulites, which develop during isothermal crystallization.

Keywords Isothermal crystallization · Morphology · Poly(3-hydroxybutyrate-*co*-3-hydroxyvalerate) · Epoxidized natural rubber

Introduction

Mixing of two or more polymers to produce blends by common processing steps is today a well-established approach for obtaining suitable materials for specific end-uses. Specific applications of biodegradable blends have drawn marked attention in offering an attractive route to further improve environmental waste management [1–5]. Poly(3-hydroxybutyrate-*co*-3-hydroxyvalerate) (PHBV) is a naturally occurring biodegradable aliphatic polyester [6]. This random copolymer displays high

C. H. Chan (✉) · H. W. Kammer
Faculty of Applied Sciences, Universiti Teknologi MARA, 40450 Shah Alam, Malaysia
e-mail: cchan_25@yahoo.com.sg

crystallinity [7, 8]. PHBV shows narrow processing window and poor mechanical properties. In this study, the copolymer is blended with epoxidized natural rubber (ENR) to toughen the polyester. Addition of an amorphous component, ENR, may influence the crystallization behavior of PHBV and the resulting morphology. Blends of PHBV and ENR form immiscible or heterogeneous systems. Mechanical properties of these blends strongly depend on developing morphologies. Interfacial chemistry and phase structure may be controlled by thermal procedures during preparation of the blends.

Recently, there are some studies on blends with PHBV. Melt blending of PHBV with 15 mol% of HV content and ethylene–vinyl acetate (EVA) with 28 mol% vinyl acetate results in immiscible systems. Blends with low EVA content (<25 wt%) behave brittle, whereas those with EVA matrix display plastic behavior [9]. Recent research by Zhang et al. [10] shows that blends of PHBV with 14 mol% of HV content and poly(epichlorohydrin-*co*-ethylene oxide) are miscible. Studies on blends of PHBV with poly(ethylene succinate) [11] as well as poly(butylene succinate) [12] and poly(ϵ -caprolactone) [13] reveal that PHBV does not form miscible systems with these polymers as evidenced by two composition independent glass transition temperatures, which correspond to those of the neat components. However, PHBV was proved to be miscible in the amorphous state with poly(ethylene oxide) (PEO) [14] and poly(vinylidene fluoride) [15].

Melt reactions between PHBV and ENR can be observed at sufficiently high temperatures. Changes in crystallization behavior and development of morphologies caused by the melt reactions between the constituents have been reported elsewhere [16]. In the present paper, we focus on crystallization and melting behavior as well as on morphologies of PHBV/ENR blends without thermally induced melt reaction.

Experimental

Materials

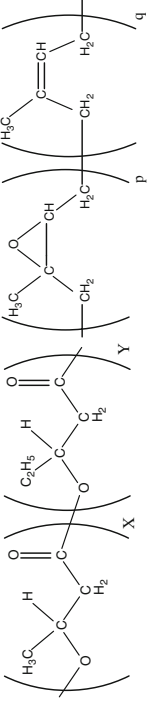
Characteristics of the polymers are given in Table 1.

PHBV and ENR were purified by filtration from chloroform (Fisher Scientific, Leicestershire, UK) solutions and precipitation in methanol (Fisher Scientific, Leicestershire, UK) afterwards. The precipitate was filtered off and dried under vacuum.

Preparation of the blends

Thin films of the blends were prepared by casting from 1% (w/w) solution of the two components in chloroform followed by evaporation of solvent at room temperature overnight and keeping afterwards the sample at 70 °C under vacuum for 48 h. Compositions of the blends ranged from 100/0 to 0/100 in steps of 10 wt%.

Table 1 Characteristics of the PHBV and ENR samples

Polymer	PHBV with 12 mol% HV	ENR 50 mol% epoxy groups
M_w (g mol ⁻¹) ^a	238,000	129,000
M_n (g mol ⁻¹) ^a	109,000	28,000
T_m (°C) ^b	161	–
T_g (°C) ^c	0	–22
ΔH_{ref} (J g ⁻¹) ^d	109 ^d	–
Molecular structure		
Supplier	Aldrich Chemical Co. (St. Louis, MO, US)	Guthrie Sdn. Bhd., Malaysia (Sungai Buloh, Malaysia)

^a Molecular masses as estimated in this work by gel permeation chromatography (PerkinElmer). Polystyrene with low polydispersity was used as standard
^b Apparent melting temperature for the neat polymer during the first heating run
^c Glass transition temperature as determined in this work
^d The melting enthalpy of 100% crystalline PHBV [17]

Differential scanning calorimetry (DSC)

PerkinElmer DSC7 (Shelton, CT, US), calibrated with indium standard, has been used for the analysis of samples under nitrogen atmosphere. A new sample was used for each DSC experiment. The samples were exposed to different thermal histories:

- I. *Isothermal crystallization.* Sample was annealed at annealing temperature (T_a) at 175 °C for 1 min, followed by cooling with a rate of 20 K min⁻¹ to the respective crystallization temperature, T_c , ranging from 105 to 112 °C, and held until complete crystallization. The half time of crystallization ($t_{0.5}$) was determined at $T_c = \text{const}$. The same procedure was applied for determination of the melting point. After crystallization for $5t_{0.5}$, samples were heated up to 175 °C with a rate of 10 K min⁻¹.
- II. *Glass transition temperature determination.* Sample was annealed at $T_a = 175$ °C for 1 min, followed by cooling with a rate of 100 K min⁻¹ to -50 °C and held for 1 min. Then, the sample was reheated up to 175 °C with a rate of 10 K min⁻¹.

Polarizing optical microscope

Morphologies of blends were studied using Image-Pro Express, which was attached to the Nikon microscope (Yokohama, Japan) equipped with a Linkam heating/cooling unit. Samples were subjected to the following thermal procedure:

- III. *Morphology.* Sample was annealed at $T_a = 175$ °C for 1 min, followed by cooling with a rate of 20 K min⁻¹ to $T_c = 120$ °C and held until complete crystallization. Micrographs were captured at $T_c = 120$ °C.

Results and discussion

Glass transition temperatures

The PHBV/ENR blends were exposed to procedure II, described in [Experimental Section](#), in order to determine the glass transition temperature (T_g). The T_g s of the PHBV/ENR blends, measured in the second heating cycle are summarized in [Fig. 1](#). Glass transition temperatures of neat PHBV and neat ENR were observed at $T_g = 0$ °C and -22 °C, respectively. Two glass transition temperatures, corresponding to that of the neat constituents, were found for blends of PHBV and ENR from 80/20 to 20/80. The two glass transitions in the blends reflect immiscibility of the constituents. We note here that after melt reaction at 234 °C it was observed only one broad glass transition, which is centered at around $T_g = -11$ °C for the 50/50 blend of PHBV and ENR [[16](#)].

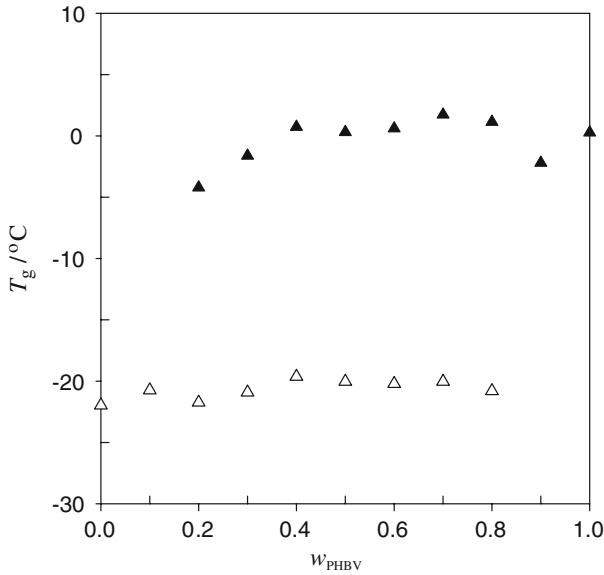


Fig. 1 Glass transition temperatures of PHBV/ENR blends measured according to thermal procedure II during reheating cycle; glass transition temperature for (*filled triangle*) PHBV and (*open triangle*) ENR

Crystallinity of PHBV

The crystallinity, X , of PHBV in PHBV/ENR blends was calculated from the enthalpy of melting, ΔH , after Eq. (1)

$$X = \left(\frac{\Delta H}{\Delta H_{\text{ref}}} \right) 100\% \quad (1)$$

where ΔH was determined after thermal procedure I and $\Delta H_{\text{ref}} = 109 \text{ J g}^{-1}$ is the reference melting enthalpy of 100% crystalline PHBV [17]. The value of ΔH_{ref} is adopted from PHBV with 10 mol% of HV content as an approximation for the PHBV with 12 mol% of HV content in this study. The half time of crystallization is the time after which 50% of the material crystallized in the isothermal crystallization process. Double melting peaks are observed for neat PHBV and other blend compositions after isothermal crystallization. Crystallization temperatures ranged from 105 to 112 °C. The double melting peaks are not well separated in most cases. Consequently, quantity ΔH refers to superposition of the melting peaks. This approximation, however, does not influence the dependence of crystallinity on blend composition. Figure 2 reveals that the amorphous component does not strongly influence the crystallinity of PHBV in the blends. Crystallization is hampered only at sufficiently high ENR contents. This behavior does not change significantly with crystallization temperature.

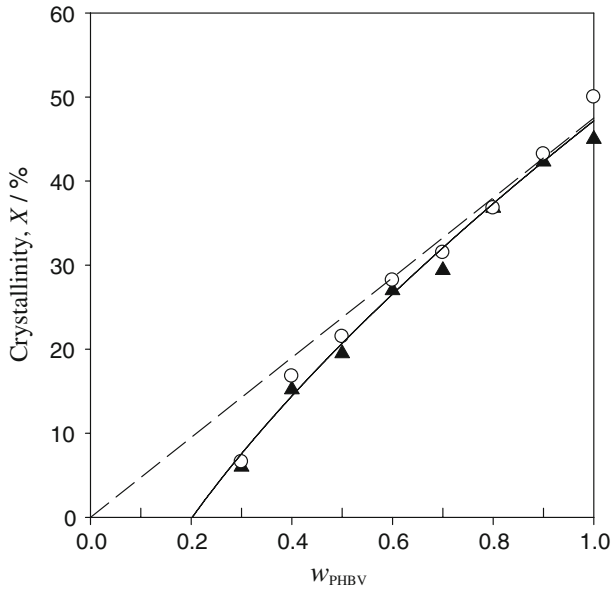


Fig. 2 Crystallinity of PHBV in PHBV/ENR blends as a function of weight fraction of PHBV after the samples were exposed to thermal procedure I. Samples were isothermally crystallized at (filled triangle) 105 and (open circle) 112 °C. The solid curve represents the regression curve of all experimental data points. The dashed curve gives the loci of constant crystallinity

Melting behavior of PHBV

Melting temperatures, T_m , of the reheating cycle were measured after the samples were crystallized isothermally for five half times at the respective T_c after thermal procedure I. The equilibrium melting temperature, T_m^0 , was determined after Hoffman–Weeks method [18]. DSC scans of selected samples are presented in Fig. 3. All the DSC thermograms exhibit two melting peaks. The lower melting peak was used for determination of apparent melting temperature since only this peak shifts with crystallization temperature.

Hoffman–Weeks plots of the PHBV/ENR blends are shown in Fig. 4. For respective blend compositions, an increasing T_m can be clearly recognized with ascending T_c indicating formation of more perfect crystals at elevated T_c . Moreover, we observe the slopes α of the Hoffman–Weeks functions $T_m(T_c)$ are constant to a good approximation with respect to varying ENR content. In thermodynamic terms, parameter α is related to the entropy change in the amorphous phase caused by crystallization. Hence, constancy of α reflects the fact that this entropy change is not influenced by ENR. The results of linear regression of Hoffman–Weeks plots are summarized in Table 2. The equilibrium melting temperature of PHBV stays constant in the blends to a good approximation.

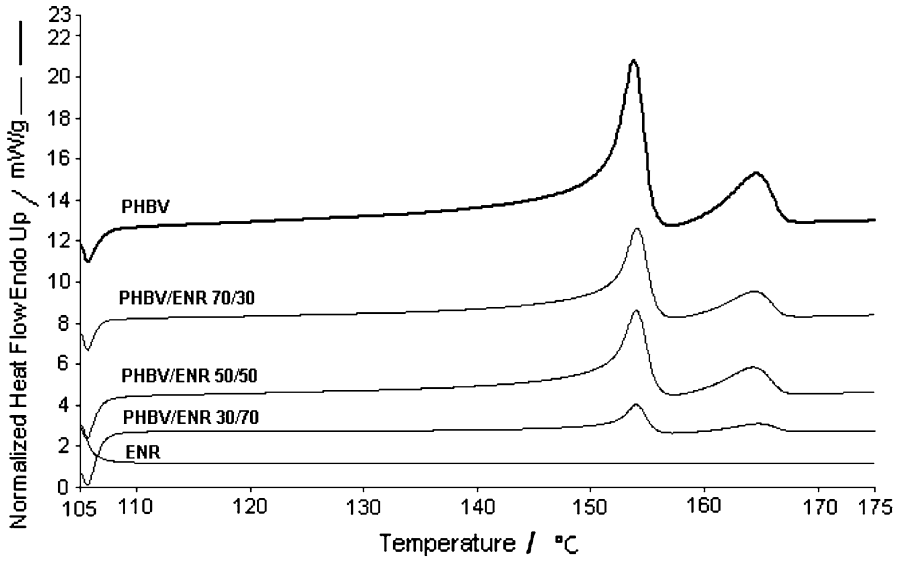


Fig. 3 DSC traces of reheating cycles after exposing PHBV/ENR samples to thermal procedure I at $T_c = 105^\circ\text{C}$. The DSC traces are displaced for better identification

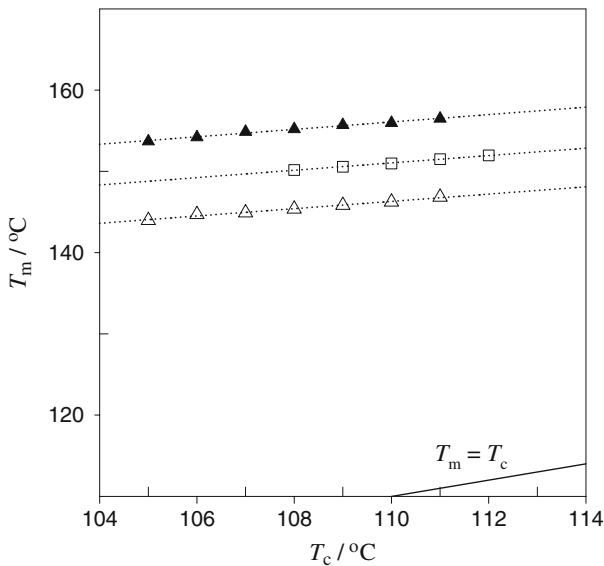


Fig. 4 Hoffman–Weeks plots for PHBV in PHBV/ENR blends (*filled triangle*) 100/0—original position, (*open square*) 70/30—displaced by -5°C and (*open triangle*) 30/70—displaced by -10°C

Table 2 Equilibrium melting temperature, T_m^0 , and correlation coefficients r of the T_m versus T_c relationships in the crystallization temperature range of 105–112 °C

Blend of PHBV/ENR	T_m^0 (°C)	α	r
100/0	194.7	0.46	0.995
70/30	194.1	0.39	0.998
50/50	194.4	0.42	0.995
30/70	194.0	0.46	0.995

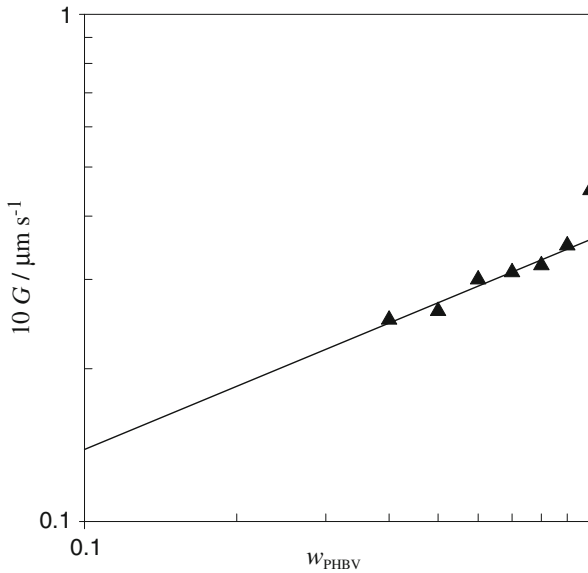


Fig. 5 Radial growth rate of PHBV spherulites as a function of weight fraction of PHBV at $T_c = 120$ °C

Spherulite growth rates

The radial growth rate, G , of PHBV spherulites was determined by polarizing optical microscope at a crystallization temperature of 120 °C. The increase of spherulite radii is strictly linear with time for all cases. The radial growth rates as shown in Fig. 5 were extracted from the slope for the plots of radius as a function of crystallization time. The error of the rates is less than 8%. Data of Fig. 5 display a power law dependence of G on blend composition

$$G = G_0 w_{\text{PHBV}}^{0.41} \quad (2)$$

After Eq. (2), the growth rate of PHBV amounts to $G_0 \approx 2.7 \mu\text{m min}^{-1}$. We note that this value of G is low as compared to poly(3-hydroxybutyrate) (PHB). For PHB, the growth rate was reported to be 12 and $8 \mu\text{m min}^{-1}$ at $T_c = 120$ °C [20] and 130 °C [21], respectively.

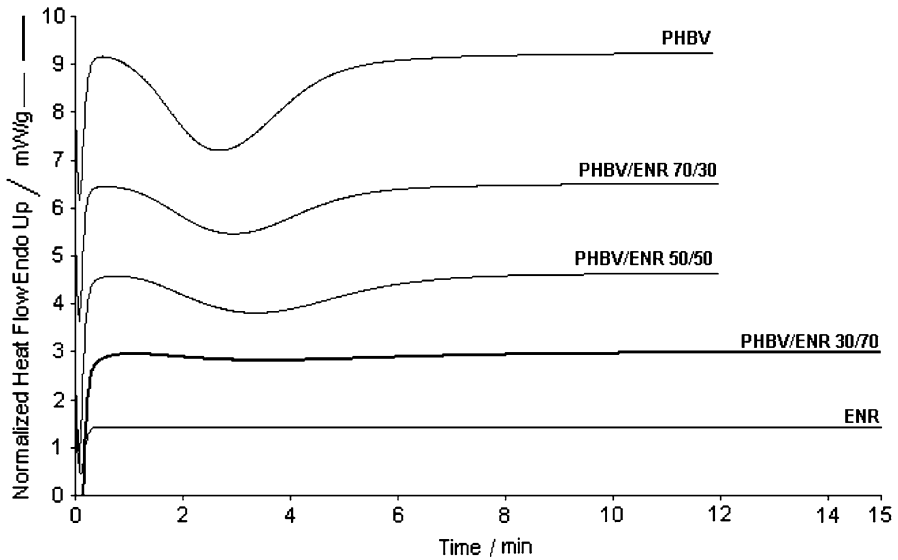


Fig. 6 DSC traces of isothermal crystallization at $T_c = 105\text{ }^\circ\text{C}$ for PHBV in the blends of PHBV/ENR after exposing samples to thermal procedure I. Curves were displaced for better identification

Kinetics of isothermal crystallization of PHBV

Isothermal crystallization experiments were carried out according to thermal procedure I, as described in the Experimental Part. Fig. 6 shows qualitatively the reduction of the crystallization rate of PHBV in blends of PHBV/ENR with increasing content of ENR at isothermal crystallization temperature, $T_c = 105\text{ }^\circ\text{C}$. In the heterogeneous system under discussion, phase boundaries or morphology of the blend might also influence the overall rate of crystallization. Therefore, we restrict application of Avrami equation [19]

$$X(t) = 1 - \exp\left[-K_A^{1/n} t\right]^n \quad (3)$$

to neat PHBV. The rate of crystallization of PHBV in blends is simply characterized by the reciprocal half time $(t_{0.5})^{-1}$, which can be defined independently of Eq. (3). In addition, results for pure PHBV may serve as reference for evaluation of crystallization of PHBV in blends. In Eq. (3), the degree of conversion, $X(t)$, is the normalized crystallinity given as the ratio of the degree of crystallinity at time, t , and the final degree of crystallinity. Quantities $K_A^{1/n}$ and n represent the overall rate constant of crystallization and the Avrami exponent, respectively. Avrami plots for PHBV are strictly linear up to conversions of 80% (correlation coefficients >0.9990). Table 3 shows Avrami coefficients for two crystallization temperatures. We note Avrami exponent $n \approx 3$.

Half times of crystallization, $t_{0.5}$, can be estimated from the DSC traces. Figure 7 exhibits decreasing rates of crystallization $(t_{0.5})^{-1}$, with ascending content of ENR. When the weight fraction of PHBV is less than 0.3, the rate of crystallization

Table 3 Avrami parameters for the kinetics of crystallization of PHBV at $T_c = 105$ and 112 °C

T_c (°C)	105	112
$K_A^{1/n}$ (min^{-1})	0.36	0.17
n	2.6	3.0
$(t_{0.5})^{-1}$ (min^{-1})	0.42	0.19

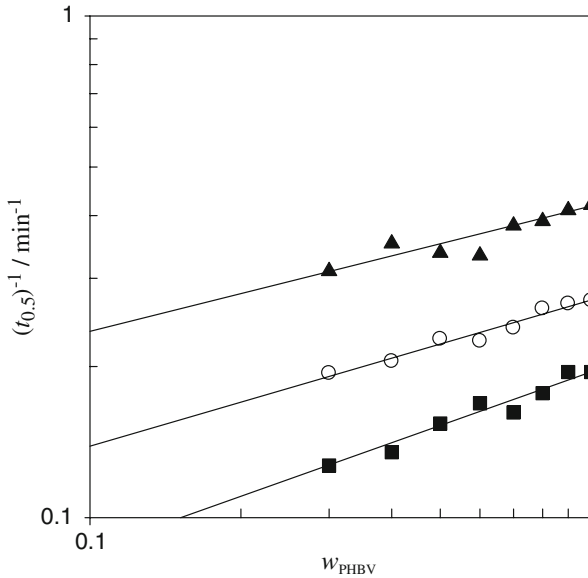


Fig. 7 Double-logarithmic plots of reciprocal half time $(t_{0.5})^{-1}$ for isothermal crystallization as a function of weight fraction of PHBV in blends of PHBV/ENR at $T_c =$ (filled triangle) 105, (open circle) 109 and (filled square) 112 °C

becomes so low that we could not detect crystallization anymore. In a heterogeneous blend, the amorphous constituent should have minor influence on the rate of crystallization as long as the crystallizable component is in excess and as long as the two constituents are largely separated. Hence, the rate of crystallization should be independent of blend composition under these conditions. After Fig. 7, we observe a power law dependence of rate of crystallization on blend composition for the PHBV/ENR blend:

$$(t_{0.5})^{-1} = (t_{0.5})_0^{-1} w_{\text{PHBV}}^x \quad (4)$$

where w symbolizes the mass fraction of PHBV. Data of Fig. 7 yield the values for exponent x as stated in Table 4. Exponent x in Table 4 is close to $1/3$, but it increases with crystallization temperature. This tendency is in accord with relationship (2) corresponding to the spherulite growth data.

Additionally to composition dependence, we will have a look to the temperature dependence of the rate of crystallization for different blend compositions. Figure 8 shows Arrhenius-like behavior of the rate constant with a slope proportional to

Table 4 Exponent x at different T_c s for PHBV in the blends after Eq. (3)

T_c (°C)	x
105	0.24
109	0.29
112	0.35

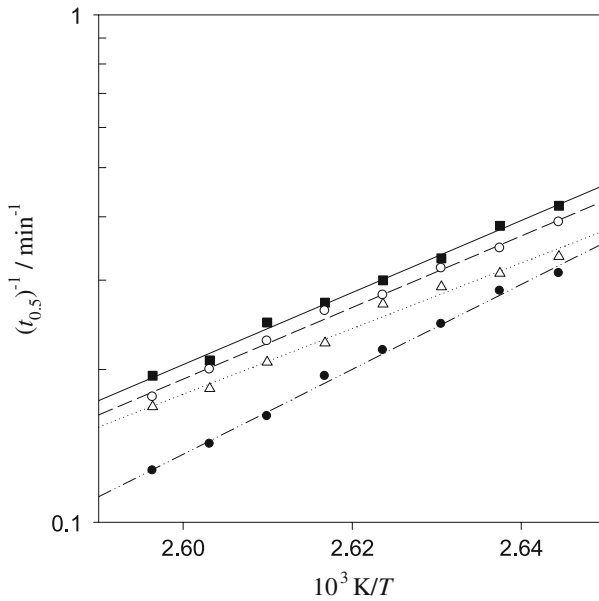


Fig. 8 Arrhenius plots of rate of crystallization for PHBV/ENR blends: (filled square) 100/0, (open circle) 80/20, (open triangle) 60/40 and (filled circle) 30/70

activation energy. One recognizes that the slope is constant to a good approximation as long as PHBV is in excess. Figure 9 underlines constancy of activation energy in blends with PHBV matrix. When PHBV becomes the dispersed phase the activation energy increases and displays huge scatter and no systematic variation with composition.

Combining the dependencies of the rate on composition as well as on temperature, one may draw the following conclusion. The overall rate of crystallization in the blend may be seen as the rate of phase separation and the rate of transport to the site of crystallization. As the constancy of activation energy shows, the rate of phase separation does not change to a good approximation with blend composition. As long as the components are sufficiently separated from each other, the rate of transport should not be influenced either. However, this is obviously not true for the blends under discussion. When dispersed regions of ENR cannot be rejected by the growing spherulite, but are intraspherulitically entrapped, then rate of crystallization may slow down with increasing ENR content as reflected

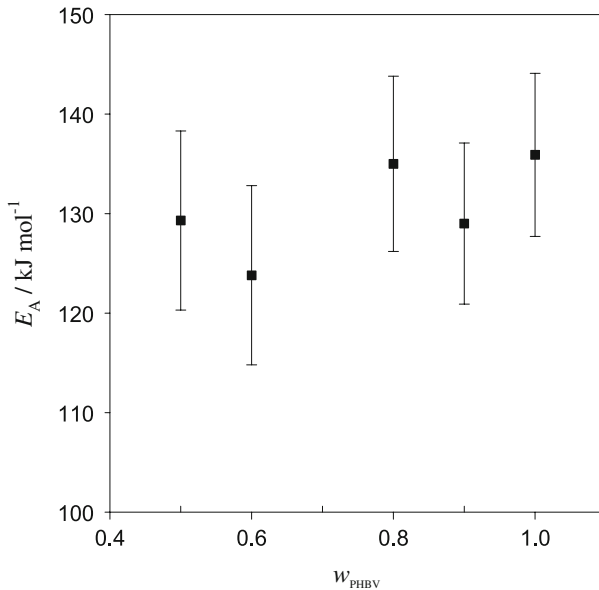


Fig. 9 Activation energy versus blend composition as calculated from the slopes of Fig. 8

in relationships (2) and (4). This conclusion is confirmed by the micrographs presented in next paragraph.

Blend morphologies

Figure 10 shows selected examples of spherulite morphologies that developed in the blends of PHBV and ENR at $T_c = 120$ °C until complete crystallization. Volume-filling spherulites grow in PHBV/ENR blends. In agreement with discussion in the previous paragraph, we note a fine intraspherulitic dispersion of ENR in PHBV. This might be caused by the higher elasticity of ENR as compared to PHBV and causes decrease in rate of crystallization with ascending ENR content since the growing front of PHBV cannot reject ENR. Similar spherulite morphologies were reported for blends of PHBV and ENR after melt reaction at 234 °C and isothermally crystallized afterwards at 50 °C [16].

Conclusion

Crystallization and melting behavior, as well as morphology have been studied for blends of PHBV and ENR. Two distinct glass transition temperatures, corresponding to that of the neat constituents, indicate immiscibility of the polymers. Only minor changes of PHBV crystallinity can be observed in blends with ENR. The rate of crystallization, on the other side, decreases with ascending content of ENR

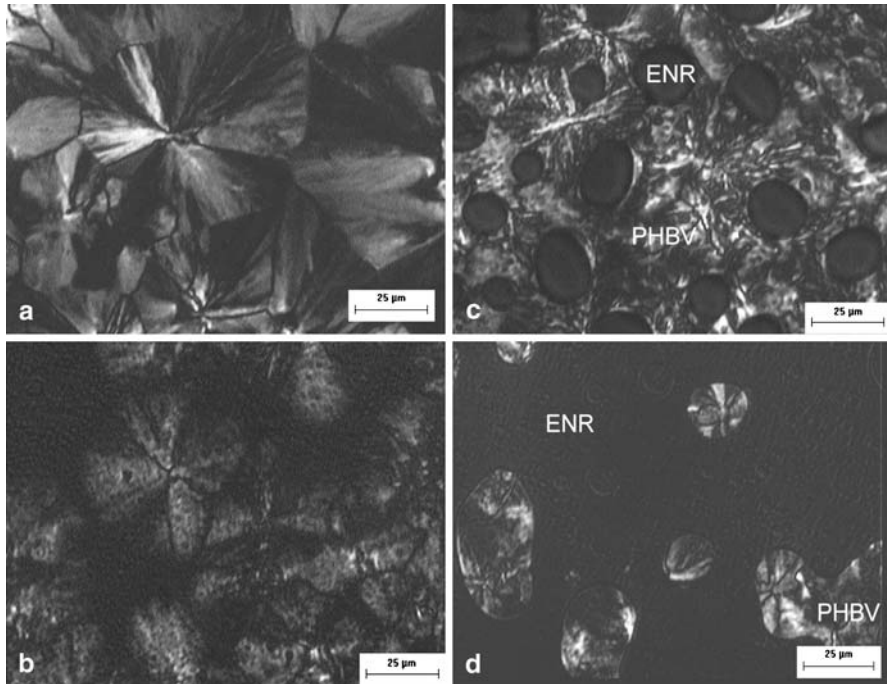


Fig. 10 Morphology of PHBV/ENR blends, isothermally crystallized at $T_c = 120$ °C after complete crystallization. Micrographs taken at 120 °C. PHBV/ENR blends: **a** 100/0, **b** 70/30, **c** 60/40 and **d** 40/60. Magnification: 40 \times . The bar corresponds to 25 μ m

according to a power law in PHBV content. This seems to be caused by fine intraspherulitic dispersion of ENR in PHBV spherulites.

Acknowledgment This work is supported by eScience research grant (03-01-01-SF0178) from Ministry of Science, Technology and Innovation (MOSTI), Malaysia.

References

1. Avella M, Martuscelli E, Raimo M (1993) The fractionated crystallization phenomenon in poly(3-hydroxybutyrate)/poly(ethylene oxide) blends. *Polymer* 34:3234–3240
2. Kumagai Y, Doi Y (1992) Enzymatic degradation of poly(3-hydroxybutyrate)-based blends: poly(3-hydroxybutyrate)/poly(ethylene oxide) blend. *Polym Degrad Stab* 35:87–93
3. Kumagai Y, Doi Y (1992) Enzymatic degradation of binary blends of microbial poly(3-hydroxybutyrate) with enzymatically active polymers. *Polym Degrad Stab* 37:253–256
4. Yoon JS, Lee WS, Kim KS, Chin IJ, Kim MN, Kim CH (2000) Effect of poly(ethylene glycol)-*block*-poly(L-lactide) on the poly[(R)-3-hydroxybutyrate]/poly(L-lactide) blends. *Eur Polym J* 36:435–442
5. Chun YS, Kim WN (2000) Thermal properties of poly(hydroxybutyrate-*co*-hydroxyvalerate) and poly(ϵ -caprolactone) blends. *Polymer* 41:2305–2308
6. Holmes PA (1985) Application of PHB—a microbially produced biodegradable thermoplastic. *Phys Technol* 16:32–36

7. Kamiya N, Sakurai M, Inoue Y, Chûjô R, Doi Y (1991) Study of cocrystallization of poly(3-hydroxybutyrate-*co*-3-hydroxyvalerate) by solid-state high-resolution carbon-13 NMR spectroscopy and differential scanning calorimetry. *Macromolecules* 24:2178–2182
8. Allegra G, Bassi IW (1969) Isomorphism in synthetic macromolecular systems. *Adv Polym Sci* 6:549–574
9. Grassner F, Owen AJ (1992) On the physical properties of BIOPOL/ethylene–vinyl acetate blends. *Polymer* 33:2508–2512
10. Zhang LL, Goh SH, Lee SY, Hee GR (2000) Miscibility, melting and crystallization behavior of two bacterial polyester/poly(epichlorohydrin-*co*-ethylene oxide) blend systems. *Polymer* 41:1429–1439
11. Miao L, Qiu Z, Yang W, Ikehara T (2008) Fully biodegradable poly(3-hydroxybutyrate-*co*-hydroxyvalerate)/poly(ethylene succinate) blends: phase behavior, crystallization and mechanical properties. *React Funct Polym* 68:446–457
12. Qui ZB, Ikehara T, Nishi T (2003) Miscibility and crystallization behaviour of biodegradable blends of two aliphatic polyesters. Poly(3-hydroxybutyrate-*co*-hydroxyvalerate) and poly(butylene succinate) blends. *Polymer* 44:7427–7519
13. Qiu ZB, Yang W, Ikehara T, Nishi T (2005) Miscibility and crystallization behavior of biodegradable blends of two aliphatic polyesters. Poly(3-hydroxybutyrate-*co*-hydroxyvalerate) and poly(ϵ -caprolactone). *Polymer* 46:11814–11819
14. Tan SM, Ismail J, Kummerlöwe C, Kammer HW (2006) Crystallization and melting behavior of blends comprising poly(3-hydroxy butyrate-*co*-3-hydroxy valerate) and poly(ethylene oxide). *J Appl Polym Sci* 101:2776–2783
15. Qiu ZB, Fujinami S, Komura M, Nakajima K, Ikehara T, Nishi T (2004) Spherulitic morphology and growth of poly(vinylidene fluoride)/poly(3-hydroxybutyrate-*co*-hydroxyvalerate) blends by optical microscopy. *Polymer* 45:4355–4360
16. Chan CH, Ismail J, Kammer HW (2004) Melt reaction in blends of poly(3-hydroxybutyrate-*co*-3-hydroxyvalerate) and epoxidized natural rubber. *Polym Degrad Stab* 85:947–955
17. Scandola M, Focarete ML, Adamus G, Sikorska W, Baranowska I, Swierczek S, Gnatowski M, Kowalczyk M, Jedlinski Z (1997) Polymer blends of natural poly(3-hydroxybutyrate-*co*-3-hydroxyvalerate) and a synthetic atactic poly(3-hydroxybutyrate). Characterization and biodegradation studies. *Macromolecules* 30:2568–2574
18. Hoffman JD, Weeks JJ (1962) Melting process and equilibrium melting temperature of polychlorotrifluoroethylene. *J Res Natl Bur Stand (A)* 66:13–28
19. Avrami M (1939) Kinetics of phase change. I. General theory. *J Chem Phys* 7:1103–1112
20. Xing PX, Dong LS, An YX, Feng ZL, Avella M, Martuscelli E (1997) Miscibility and crystallization of poly(β -hydroxybutyrate) and poly(*p*-vinylphenol) blends. *Macromolecules* 30:2726–2733
21. Chan CH, Kummerlöwe C, Kammer HW (2004) Crystallization and melting behavior of poly(3-hydroxybutyrate)-based blends. *Macromol Chem Phys* 205:664–675